ORIGINAL ARTICLE

Cortical spreading depolarization stimulates gliogenesis in the rat entorhinal cortex

Anja Urbach[1], Judith Brueckner[1] and Otto W Witte[1,2]

Recently, we showed that cortical spreading depolarizations (CSDs) are a potent trigger of hippocampal neurogenesis. Here, we evaluated CSD-induced cytogenesis in the entorhinal cortex (EC), which provides the major afferent input to the dentate gyrus. Cortical spreading depolarizations were induced by epidural application of 3 mol/L KCl, controls received equimolar NaCl. Cytogenesis was analyzed at different time points thereafter by means of intraperitoneal 5-bromodeoxyuridine injections (day 2, 4, or days 1 to 7) and immunohistochemistry. Recurrent CSD significantly increased numbers of newborn cells in the ipsilateral EC. The majority of these cells expressed glial markers. Microglia proliferation was maximal at day 2, whereas NG2 glia and astrocytes responded for a prolonged period of time (days 2 to 4). Newborn glia remained detectable for 6 weeks after CSD. Whereas we furthermore detected newborn cells immunopositive for doublecortin, a marker for immature neuronal cells, we found no evidence for the generation of new neurons in the EC. Our results indicate that CSD is a potent gliogenic stimulus, leading to rapid and enduring changes in the glial cellular composition of the affected brain tissue. Thus, CSD facilitates ongoing structural remodeling of the directly affected cortex that might contribute to the pathophysiology of CSD-related brain pathologies.

INTRODUCTION

Cortical spreading depolarization (CSD) is characterized by a wave of neuronal and glial depolarization and near-complete breakdown of the neuronal ion gradients that slowly propagates from a trigger point across the ipsilateral cortical gray matter.[1,2] It is associated with changes in cerebral blood flow and energy metabolism. In tissue with preserved brain electrical activity, CSD causes spreading depression of the spontaneous activity, but CSD can also occur in the absence of brain activity. There is strong experimental and clinical evidence that CSD is involved in the pathophysiology of neurologic disorders like ischemic and hemorrhagic stroke, traumatic brain injury, and migraine.[2,3] The acute pathologies among them trigger a robust glial response in perilesional but also remote brain tissue, leading to activation and proliferation of macroglial and microglial cells.[4–8] They furthermore induce the generation of new neurons from the two major neurogenic niches of the adult brain, the subventricular zone and the dentate subgranular zone.[7,9] Previously, we showed that recurrent CSD activates dentate neurogenesis to a similar degree, indicating CSD as a mechanism underlying injury-induced neurogenesis.[10] Further experimental evidence suggests that CSD is involved in the activation and proliferation of glial cells in cortical areas remote to an injury: it provokes the expression of markers characteristic for reactive astrogliosis and microgliosis like GFAP, nestin, CD68, and CD74,[11–13] and enhances the number of dividing cells that coexpress GFAP or NG2.[14,15]

On the basis of these findings, we sought to determine the capacity of CSD to change cell proliferation and to expand newborn glia of particular lineage in the entorhinal cortex (EC) of adult rats. Entorhinal cortex was analyzed because our preliminary studies revealed that in comparison with neocortical areas (e.g., parietal cortex) the allocortex (e.g., EC and perirhinal cortex) showed the most pronounced proliferative response to CSD. We provide evidence that, in the EC, CSD is a potent gliogenic stimulus, with microglia primarily reacting at early stages, whereas the populations of astrocytes and NG2 glia respond for a prolonged period of time. There was no evidence for CSD-induced *in vivo* cortical neurogenesis.

MATERIALS AND METHODS

Animals, Surgery, and 5′-Bromodeoxyuridine Injections

All procedures involving living animals were performed in accordance with the EC directive 86/609/EEC guidelines for animal experiments and were approved by the Governmental Animal Care Committee (Thüringer Landesamt für Lebensmittelsicherheit und Verbraucherschutz; no. 02-012/07). Experiments are reported in accordance with the ARRIVE guidelines. Animals were housed under a 12-hour light/dark cycle with *ad libitum* access to food and water. A total of 32 male Wistar rats (280 to 320 g, ~3 months old) were used for the experiments. Surgery was performed as described earlier.[10] Briefly, rats were anesthetized with 2.5% isoflurane in 60/30 l N_2O/O_2 and fixed in a stereotactic frame. Rectal temperature was kept constant at 37 ± 0.5°C. Two craniotomies (Bregma +2 mm, 2 mm lateral and Bregma − 5 mm, 3 mm lateral; diameter 1.8 mm) were made above the left hemisphere leaving the dura mater intact. An Ag/AgCl-reference electrode was placed subcutaneously in the neck. A glass recording electrode (2 to 4 MΩ) filled with artificial cerebrospinal fluid (120 NaCl, 2 $CaCl_2$, 5 KCl, 1.8 $MgCl_2$, 10 HEPES, 1.25 NaH_2PO_4, and 10

[1]Hans Berger Department of Neurology, Jena University Hospital, Jena, Germany and [2]Center for Sepsis Control and Care, Jena University Hospital and Friedrich Schiller University Jena, Jena, Germany. Correspondence: Dr A Urbach, Hans Berger Department of Neurology, Jena University Hospital, Erlanger Allee 101/FZL, Jena 07747, Germany.
E-mail: anja.urbach@med.uni-jena.de

Glucose; in mmol/L) containing an Ag/AgCl wire was placed on the dura at the anterior position and connected to a high impedance amplifier (EXT-08, NPI, Tamm, Germany). Amplified signals (100x) were continuously digitized and stored on a PC equipped with an A/D converter (CED 1401, Cambridge Electronic Design Ltd., Cambridge, England) and Spike 2 software (Cambridge Electronic Design Ltd.) to record the electrocorticogram and direct current potential. Recordings were allowed to stabilize, while anesthesia was successively reduced to 1.5% isoflurane. Then, a small swab soaked with 3 mol/L KCl (CSD group) or 3 mol/L NaCl (sham) was applied to the dura above the occipital cortex and renewed every 15 minutes. After recording of 7 ± 2 CSDs (usually in the range of 100 to 120 minutes; Supplementary Figure 1, Supplementary Table 1) the swab was removed, craniotomies were rinsed with artificial cerebrospinal fluid and sealed with bone wax.

We used the thymidine analog 5′-bromodeoxyuridine (BrdU, Sigma-Aldrich, St Louis, MO, USA; 50 mg/kg body weight) to label proliferating cells. Rats were randomly assigned to three groups with different BrdU injection schemes and survival times (Supplementary Figure 2). Two groups received three intraperitoneal injections of BrdU every 8 hours at either day 2 (CSD: $n = 5$, sham: $n = 4$) or day 4 after surgery (CSD: $n = 6$, sham: $n = 4$) and were allowed to recover until the next day. Another group was injected with BrdU every 12 hours for 7 consecutive days starting the day after surgery. These rats were killed at day 42 (CSD: $n = 9$, sham: $n = 4$).

Immunohistochemistry

5′-Bromodeoxyuridine immunohistochemistry was conducted on $40 \mu m$ slices of 4% PFA-fixed brains according to the standard peroxidase (ABC) method. Every sixth section was rinsed in Tris-buffered saline, blocked for 30 minutes in 0.6% H_2O_2, denatured in 2 N HCl at 37°C for 30 minutes and neutralized for 10 minutes in 0.1 mol/L borate buffer followed by a blocking step in Tris-buffered saline plus (0.1% triton, 2% milk powder, 2% bovine serum albumin, 3% donkey serum). Primary rat anti-BrdU antibody (1:500; AbD Serotec, Oxford, UK) was applied overnight at 4°C. Then, slices were treated with secondary antibody (biotinylated donkey anti-rat IgG 1:500; Dianova, Hamburg, Germany) for 2 hours and incubated in Vectastain ABC-peroxidase kit (Vector Laboratories, Burlingame, CA, USA) for 1 hour. Signals were visualized by diaminobezidine staining (Sigma-Aldrich).

Immunofluorescence

For coexpression studies, we used triple immunofluorescence with antibodies against BrdU (rat, 1:500; AbD Serotec), the early neuronal marker DCX (goat, 1:200; Santa Cruz, Dallas, TX, USA), the neuronal marker NeuN (mouse, 1:500; Chemicon, Billerica, MA, USA), the astrocytic markers S100ß (rabbit, 1:2,500; Swant, Marly, Switzerland) and GFAP (guinea pig, 1:500; Advanced ImmunoChemical, Long Beach, CA, USA), the NG2-cell marker NG2 (rabbit, 1:500; Chemicon), the oligodendrocyte marker CNPase (mouse, 1:500; Abcam, Cambridge, UK) and nestin (mouse, 1:500; BD Biosciences, Heidelberg, Germany). Microglia was identified using TRITC-conjugated lectin from *Bandeiraea simplicifolia* (1:200; Sigma-Aldrich) or Iba1 (rabbit 1:1,000; Wako, Neuss, Germany). Every twelfth section was stained as described above except the H_2O_2 blocking step. Binding of primary antibodies was detected using species-specific secondary antibodies (1:250) labeled with different fluorochromes: Rhodamine-conjugated donkey anti-rat (Dianova), Alexa 488-conjugated goat anti-guinea pig (Molecular Probes, Carlsbad, CA, USA), Alexa 488-conjugated donkey anti-rabbit (Molecular Probes), Cy5-conjugated donkey anti-mouse (Dianova), and Cy5-conjugated donkey anti-goat (Dianova).

Cell quantification

5′-Bromodeoxyuridine-positive cell numbers were quantified throughout the lateral EC using an unbiased stereological method (optical fractionator, StereoInvestigator; Micro Brightfield, Williston, VT, USA). In all cases, the experimenter was blinded to the animal group assignments. Every sixth section was analyzed from Bregma − 4.8 to − 6.8 according to Paxinos & Watson coordinates (Supplementary Figure 3). Contours of the region of interest were drawn using a ×1.25 objective and quantification was performed at a magnification of ×630. Grid and counting frame dimensions were adjusted depending on the density of BrdU-positive cells to obtain at least 1 to 3 counts on average per dissector. Cell counts were estimated in 200 to 400 frames per hemisphere. These parameters remained constant within groups. The average thickness of mounted sections was $14 \mu m$ and 10% guard zones were defined to avoid oversampling. The reference volume was calculated by multiplying the traced areas of each hemisection

with the section interval (6) and the section thickness ($40 \mu m$). Data were expressed as the number of BrdU-labeled cells per mm^3.

Cell phenotypization

For phenotypization, random fields in the EC of every twelfth section were scanned as z-stacks by confocal laser scanning microscopy (LSM 510 META, Zeiss, Jena, Germany). In total, the phenotypes of 50 to 60 BrdU-positive cells were determined per hemisphere. The percentage of colabeled cells was calculated and absolute numbers of the different cell populations were obtained by multiplying the percentage with total numbers of BrdU-positive cells per mm^3.

Statistical methods

We applied nonparametric statistics to analyze differences between two data sets and reported data as median with interquartile ranges (IQR). Both were calculated using the explorative data analysis tool of SPSS 21 (IBM SPSS statistics, Ehningen, Germany). Dependent variables (ipsi versus contra) were furthermore compared using the Wilcoxon test and independent variables (sham versus CSD) using the Mann–Whitney test (both two-tailed). A level of $P < 0.05$ was considered as statistically significant.

RESULTS

5′-Bromodeoxyuridine-positive nuclei of different morphology were observed throughout all layers of the lateral EC of sham and CSD animals (Figure 1, Supplementary Figure 4). Cortical spreading depolarization increased the density of BrdU-positive cells in the ipsilateral EC (Figure 1, Table 1): after pulse labeling with BrdU on the day preceding analysis we detected 188% (day 3, $P = 0.016$; Figure 1A) to 157% (day 5, $P = 0.01$; Figure 1B) more BrdU-positive nuclei in the EC of CSD rats as compared with sham. When BrdU was injected during the first week after CSD and immunodetection was performed 6 weeks thereafter, BrdU-positive nuclei in the ipsilateral EC were increased by 339% ($P = 0.003$). Contralateral to the CSD we detected a 57% increase in BrdU-positive cells at day 3 ($P = 0.014$) while the other time points revealed no significant differences relative to sham EC (Figures 1A to 1C, Table 1).

To examine the phenotype of newborn cells, we performed multiple immunofluorescence labeling with antibodies against BrdU and different glia- and neuron-specific antigens. Generally, CSD increased the density of newborn astroglia, microglia, and NG2 glia (Table 1). It furthermore shifted the relative frequencies of different glia cell types within the population of newborn cells toward microglia and astroglia (Supplementary Table 2). Nonetheless, the majority of newborn cells in the EC were NG2 positive, regardless of group and time point. In terms of absolute numbers, CSD induced an expansion of the newborn NG2-positive cell population at all time points investigated (Table 1, Figure 2A). The BrdU/NG2-positive cells displayed a complex morphology with multiple long and ramified processes radiating from the soma, characteristic of cortical NG2 glia/synantocytes (Figure 2A). In sham EC and contralateral to the CSD the NG2-positive cell population comprised 72% to 87% of all BrdU-positive cells (Supplementary Table 2). Due to CSD, the percentage of newborn NG2 glia rapidly decreased to 48% of the BrdU-positive population (day 3: $P = 0.032$), while returning to baseline (sham) levels on day 5 (81%, $P = 0.762$; Supplementary Table 2). When we evaluated the cell population born during the first week after CSD at day 42, NG2 cells again comprised only 28% of all BrdU-positive cells ($P = 0.02$; Supplementary Table 2). By the same time, we detected BrdU/CNPase-double positive cells that appeared more abundant in the CSD cortex as compared with the contralateral or sham cortex (not quantified; Supplementary Figure 7). Together, these data indicate that CSD changes the relative share of newborn NG2 cells only within a very short early time window but with long-term consequences on the composition of the newborn glia pool.
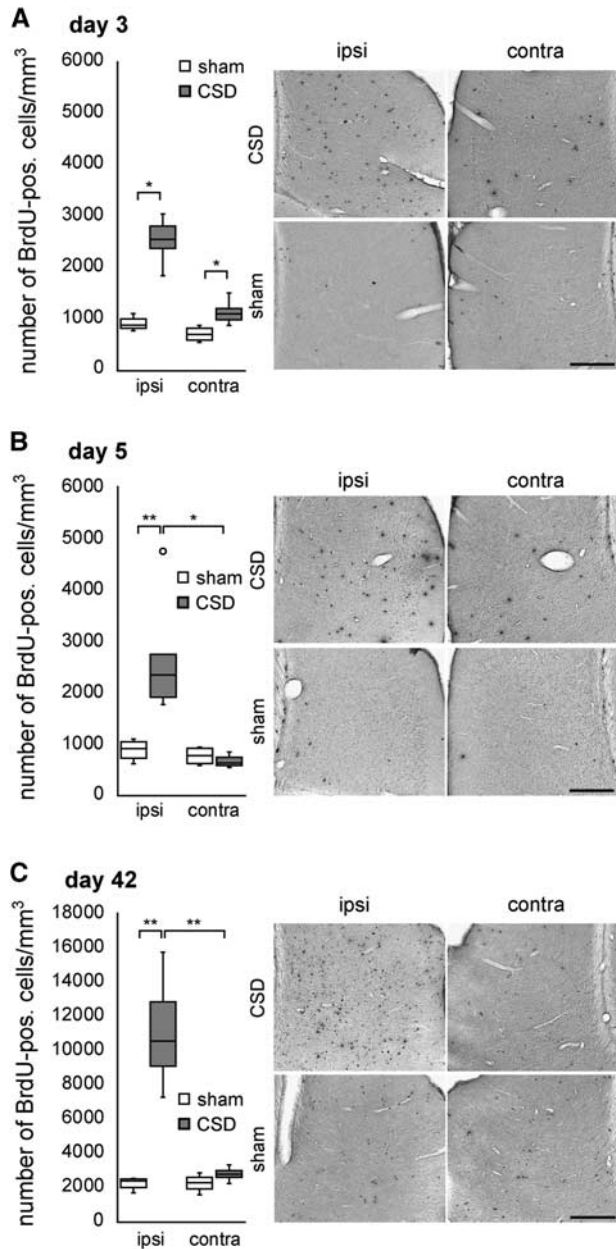
Figure 1. Quantification of newborn cells in the lateral entorhinal cortex (EC) of cortical spreading depolarization (CSD) and sham animals (cells per mm³; median with interquartile ranges (IQR), circle indicates an outlier). CSD increased 5′-bromodeoxyuridine (BrdU)-positive cell numbers at all time points that were assessed (**A** to **C**). *$P < 0.05$ or **$P < 0.01$.

Newborn microglia was only sparcely distributed in sham animals and the EC contralateral to the CSD. After CSD we found a rapid increase in the percentage (Supplementary Table 2) and density (Table 1, Figure 2B) of BrdU/lectin-double labeled microglia in the ipsilateral EC, which was most prominent at day 3 ($P = 0.016$). At day 42, the percentages of newborn microglia in CSD and sham EC were no longer distinguishable. However, the density of newborn microglia was still increased in CSD cortex ($P = 0.006$), but it did not exceed the value of day 3. This indicates either that the microglial response is very short or that part of the microglia born during the first days after CSD subsequently died. As opposed to the other glial populations numbers of newborn

microglia were slightly increased in the contralateral cortex at day 3 ($P = 0.032$). This increase in proliferating microglia was accompanied by only mildest morphologic signs of activation. Cortical spreading depolarization elicited an upregulation of Iba1 and a hypertrophy of cell bodies, but microglia still appeared ramified irrespective whether they were BrdU positive or negative (Figure 2B, Supplementary Figure 5).

To identify newborn astrocytes, we performed double labeling against BrdU and GFAP or S100ß. As with microglia, BrdU/GFAP-positive cells were almost absent in the EC contralateral to the CSD and in sham animals. Cortical spreading depolarization consistently increased relative and absolute numbers of these cells throughout the ipsilateral EC (Table 1, Supplementary Table 2, Figure 3B) with the percentage of newborn BrdU/GFAP-positive astrocytes ranging between 10% (day 3) and 6% (day 42). In the long term, the density of newborn GFAP-positive astrocytes increased by >20-fold (day 42, $P = 0.003$; Table 1). By contrast, BrdU/S100ß-colabeled cells were completely absent from sham EC. Cortical spreading depolarization increased the population of newborn cells coexpressing S100ß rapidly, even if a significant difference was detected only at day 42 ($P = 0.034$ relative to sham; Table 1, Supplementary Table 2, Figure 3A). At this time, the density of BrdU/S100ß-colabeled cells was similar to or even slightly exceeded that of BrdU/GFAP-colabeled cells, while it was much lower at days 3 and 5, indicating that the expression of S100ß in newborn glia was delayed. Furthermore, CSD changed the morphology of ipsilateral astrocytes toward more reactive characteristics, with hypertrophic cell bodies, thicker processes, and a higher GFAP expression as compared with sham (Supplementary Figure 6A). To further characterize the population of newborn astrocytes, we performed triple-immunofluorescence with antibodies against BrdU, GFAP, and nestin. Nestin was virtually absent in BrdU-positive cells of sham animals and contralateral to the CSD. At days 3 and 5, the percentage and density of BrdU/nestin-positive cells were significantly increased in the ipsilateral EC of CSD animals (Figure 3C, Table 1, Supplementary Table 2), and nestin was expressed in the majority of BrdU/GFAP-positive cells (day 3: 61%, day 5: 97%; data not shown). The BrdU/GFAP/nestin-triple-positive cells displayed the morphology of reactive astrocytes with features described above (Figure 3D). At day 42, nestin expression returned to control levels and was no more detectable in newborn astrocytes (Supplementary Figure 6B and C).

A subset of BrdU-positive cells in the EC of all groups was immunoreactive for the immature neuronal marker DCX (Figure 4A). These cells typically exhibited a small soma with few processes and were located in all layers of the EC except layer II, where we found many BrdU-negative DCX-expressing cells. Triple-immunofluorescence against BrdU, DCX, and NG2 revealed that newborn DCX-positive cells frequently coexpressed NG2 (Figure 4B; no quantification). Cortical spreading depolarization significantly increased the density of BrdU/DCX-positive cells on day 5 and day 42 relative to contralateral EC ($P = 0.031$ and $P = 0.039$, respectively), and on day 42 relative to sham EC ($P = 0.003$; Table 1, Figure 4A). Nevertheless, the percentage of newborn cells expressing DCX was transiently decreased in the EC ipsilateral to CSD as compared with sham (day 5: $P = 0.019$, Supplementary Table 2). We never observed colocalization of BrdU and the mature neuronal marker NeuN (Table 1, Supplementary Table 2, Figure 4C). 5′-Bromodeoxyuridine-positive cells were frequently observed adjacent to NeuN-positive cells, giving the appearance of satellite cells (Figure 4C′).

DISCUSSION

Our studies show that CSD triggers an extensive, temporally distinct hyperplasia of microglia, astrocytes as well as NG2 cells in the EC, with microglia showing the most rapid and vigorous

Table 1. Absolute numbers of newborn cell types per mm^3 ($P < 0.05$ significance compared with sham* or contralateral cortex§)

|	3 Days		5 Days		42 Days	
	Ipsilateral median (IQR)	Contralateral median (IQR)	Ipsilateral median (IQR)	Contralateral median (IQR)	Ipsilateral median (IQR)	Contralateral median (IQR)
	($n = 5$)		($n = 6$)		($n = 9$)	
CSD						
BrdU$^+$	2,550.3 (818.0)*	1,104.9 (424.5)*	2,347.8 (1367.1)*§	634.9 (191.3)	10,553.6 (5149.3)*§	2,796.5 (639.3)
DCX$^+$	304.7 (380.9)	158.6 (120.9)	534.7 (438.7)§	158.1 (86.1)	727.5 (1219.7)*§	498.3 (397.9)
NeuN$^+$	—	—	—	—	0.0 (0.0)	0.0 (0.0)
S100ß$^+$	153.0 (174.1)	0.0 (31.9)	21.7 (147.1)	0.0 (2.9)	633.2 (1752.0)*§	0.0 (82.7)
GFAP$^+$	224.7 (156.8)*	39.6 (48.1)	108.0 (477.5)*	23.7 (56.8)	570.3 (1041.4)*§	52.3 (150.0)
Nestin$^+$	147.6 (192.1)*	0.0 (9.9)	112.35 (455.3)*§	0.0 (0.0)	—	—
NG2$^+$	1,139.4 (604.3)*	842.4 (336.3)	1,773.7 (1092.0)*§	525.2 (125.1)	2,911.6 (1927.4)*§	1,857.1 (709.0)
Lectin$^+$	816.0 (805.9)*	79.3 (74.3)*	195.0 (410.5)*§	21.2 (74.5)	452.6 (1184.7)*§	45.3 (147.4)
	($n = 4$)		($n = 4$)		($n = 4$)	
Sham						
BrdU$^+$	885.3 (259.8)	702.9 (280.0)	914.6 (398.3)	780.3 (322.1)	2,405.4 (652.0)	2,314.8 (975.4)
DCX$^+$	214.9 (70.0)	57.3 (45.5)	351.7 (87.0)	166.1 (104.6)	265.3 (211.9)	479.9 (756.4)
NeuN$^+$	—	—	—	—	0.0 (0.0)	0.0 (0.0)
S100ß$^+$	0.0 (0.0)	0.0 (0.0)	0.0 (0.0)	0.0 (0.0)	0.0 (0.0)	0.0 (0.0)
GFAP$^+$	9.0 (54.5)	0.0 (39.6)	32.2 (79.2)	23.0 (77.6)	25.4 (86.9)	38.8 (38.6)
Nestin$^+$	0.0 (0.0)	0.0 (13.2)	0.0 (0.0)	0.0 (0.0)	—	—
NG2$^+$	613.8 (201.7)	586.2 (341.7)	721.8 (342.5)	682.8 (239.9)	1504.4 (653.8)	1669.3 (750.9)
Lectin$^+$	53.16 (82.8)	15.5 (60.5)	9.9 (21.4)	0.0 (24.9)	57.7 (119.9)	0.0 (47.9)

BrdU, 5′-bromodeoxyuridine; IQR, interquartile ranges.
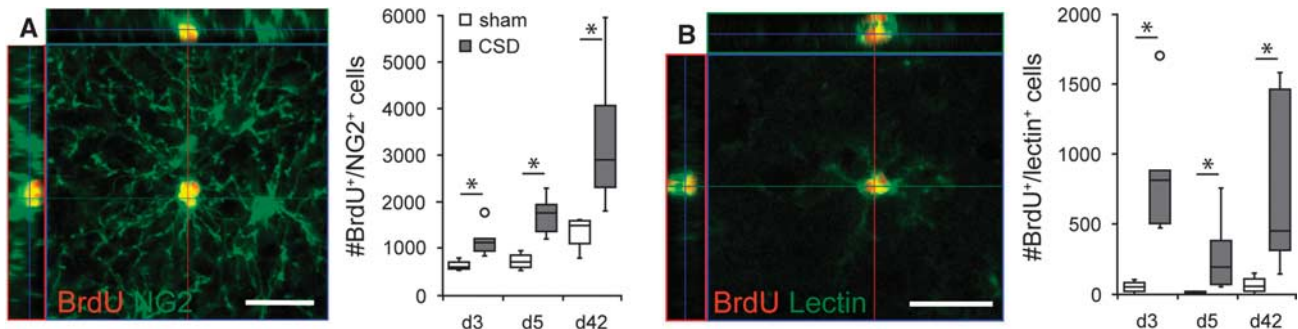
Figure 2. Confocal images and numbers (cells per mm^3; median with interquartile ranges (IQR), circles indicate outliers) of newborn NG2 glia (**A**) and microglia (**B**). Images were taken from d3 sections of ipsilateral CSD-EC. Scale bars: 20 μm, *$P < 0.05$. CSD, cortical spreading depolarization; EC, entorhinal cortex.

proliferative response. These excessively generated glial cells could be detected for more than a month, indicating that CSD has enduring consequences on the affected EC.

Microglial cells are the resident immune cells of the CNS. With their highly dynamic processes they continuously survey the microenvironment, thus being the first cells activated in response to tissue injury.[16] Previous studies revealed that CSD can induce an activated phenotype, including microglial hypertrophy and the expression of MHC class II antigens.[17] We confirmed this and now show that these changes are accompanied by a massive (approximately ninefold) expansion of the newborn microglial cell population. The response in the EC was maximal as early as at day 2 and already decreased at day 4, resembling time courses observed in remote areas after acute brain injuries.[6] The new microglia may originate either from proliferation of resident microglia or from monocytic cells recruited from the blood stream, which is frequently observed due to injuries related to breakdown of the blood–brain barrier.[16] The rapid occurrence of pairs of new

microglia with highly ramified processes argues in favor of an origin from resident microglia.

Upon CSD, astrocytes in the EC displayed typical hallmarks of reactive astrocytosis. Although it was not systematically determined, we found that astroglia transiently became hypertrophic and upregulated the intermediate filaments GFAP and nestin. Similar observations were made in the neocortex during the first 2 weeks after CSD.[12,13] More importantly, CSD strongly increased ipsilateral numbers of newborn astrocytes and in particular these new astrocytes reexpressed nestin. The astrocytic response appears to be slower and longer than that of microglia. Most likely, the new astroglia originated from mature protoplasmic astrocytes, which are the major source of reactive astrocytes in the postnatal brain.[18] Indeed, we found duplets of newborn astrocytes immediately after BrdU labeling supporting this assumption. However, there is line of evidence suggesting that a subset of gray matter reactive astrocytes may be derived from NG2 glia[19] and a recent study indicated that this may also occur after CSD.[15] Overall, our observations closely resemble the features of a severe
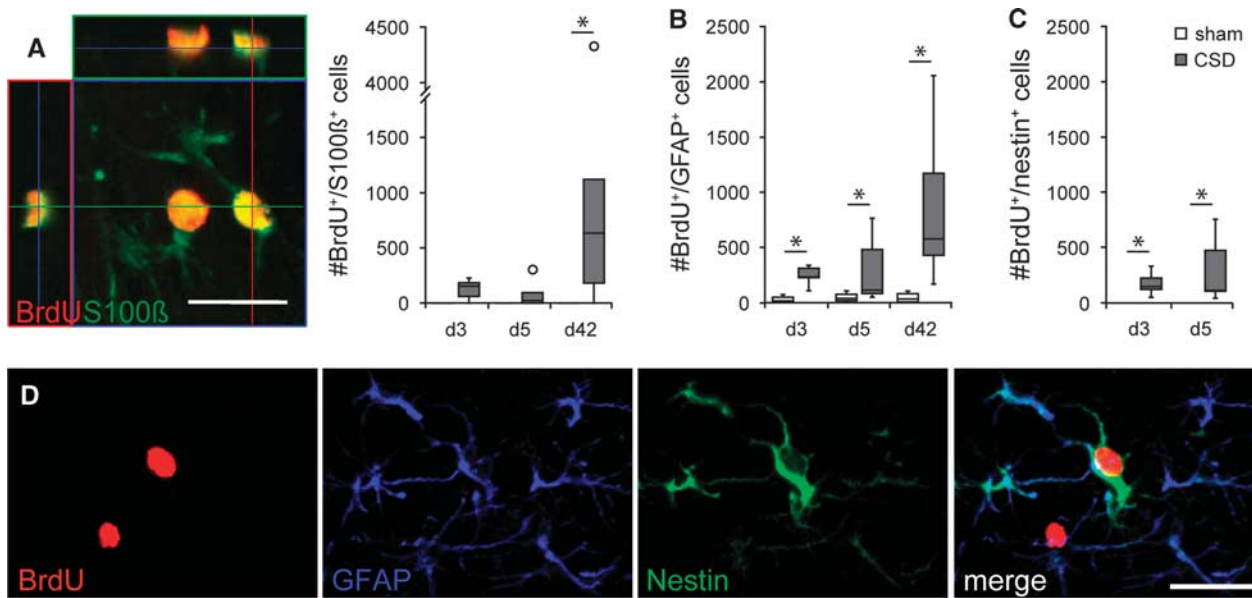
Figure 3. Confocal images and numbers (cells/mm³; median with interquartile ranges (IQR), circles indicate outliers) of newborn astroglia. (**A**) Newborn S100ß-positive cells and (**B** to **D**) newborn cells expressing GFAP and/or nestin. Images were taken from d3 sections of ipsilateral CSD-EC. Scale bars: 20 μm, *P < 0.05. CSD, cortical spreading depolarization; EC, entorhinal cortex.
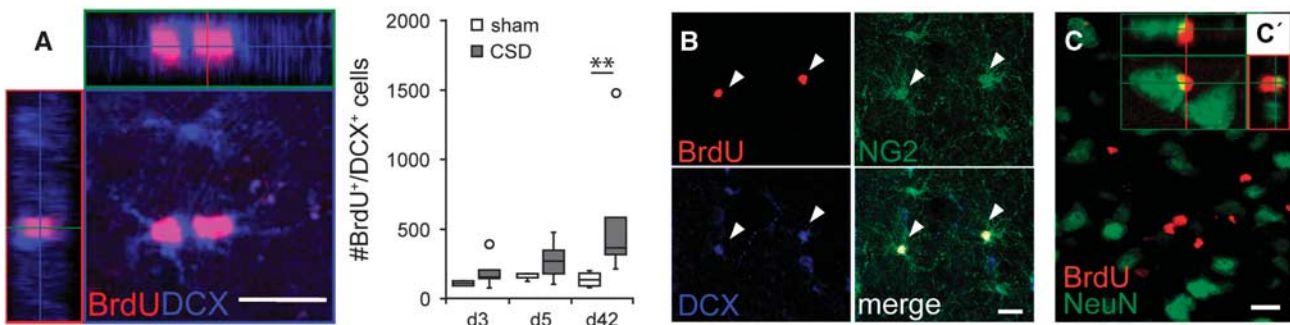

Figure 4. Phenotypization of newborn cells using neuronal markers. (**A**) Newborn DCX-positive cells (cells per mm³; median with interquartile ranges (IQR), circles indicate outliers), (**B**) NG2/DCX-double positive cells, and (**C**) z-stack projection of a d42 section double-labeled against 5´-bromodeoxyuridine (BrdU) and NeuN, and (**C´**) an BrdU-positive satellite cell tightly apposed to a neuron. Images (**A**) and (**B**) were taken from d3 sections. Scale bars: 20 μm, *P < 0.05. CSD, cortical spreading depolarization.

diffuse reactive astrogliosis as described by Sofroniew and Vinters.[8]

NG2 cells are the major cell type that, in the intact brain, constitutively proliferates outside the neurogenic niches.[20] Consistently, we found most of newborn cells in sham and contralateral EC expressing NG2. As with related pathologic conditions,[21] absolute numbers of newborn NG2 cells rapidly increased in response to CSD. A subpopulation of newborn NG2 glia coexpressed DCX. Previous studies showed that these DCX/NG2-double positive cells are the most abundant among the proliferating cells in the healthy neocortex.[22] Congruously, also the numbers of newborn DCX cells were increased in CSD cortex. The fate of these cells is unclear. DCX/NG2-double positive cells can either produce progeny of the same phenotype or differentiate into DCX-positive/NG2-negative or DCX-negative/NG2-positive cells, and are thus assumed to be the multipotent progenitor cells of the cortex.[22] DCX is a marker of cells committed to the neuronal linage, and there is evidence that under certain pathologic conditions the cortex generates few new neurons.[23]

However, we identified all new cells as nonneuronal even at 6 weeks after BrdU injection, suggesting that CSD is not sufficient to change the permissiveness of the EC to adult neurogenesis. However and consistent with the function of NG2 glia as oligodendrocyte precursors,[19,20] a subset of BrdU-positive cells at day 42 also expressed CNPase, indicating that new oligodendrocytes were generated. This population of newborn oligodendrocytes might account for the residual BrdU-positive cells that could not be classified with the neuronal and glial markers used in the present study. Further investigations have to be to evaluate the extent and possible implications of oligodendrogenesis after CSD.

Albeit a number of studies examined cell proliferation and differentiation in the cerebral cortex after stroke and other CSD-associated neuropathologies,[4–8] there are only few studies on the neuro- and gliogenic response after CSD, systematic investigations are virtually lacking. In two studies of the same group, prolonged CSD increased the number of mitotic cells and new TujI-positive neuronal cells in the subventricular zone and neocortex.[14,24]

We discovered CSD as potent activator of neurogenesis in the hippocampal neurogenic niche.[10] Recently, Tamura *et al*[15] studied the impact of CSD on temporal cortex gliogenesis. At 28 days after CSD, they basically found an expansion of newborn microglia, numbers of new astrocytes and NG2 cells were only subtly increased. Thus, the pattern of glial response they detected was different from ours. This might be related to differences in the applied BrdU injection protocols or to a region specific diversity in the proliferative response of the affected cortex. The latter assumption is supported by our preliminary experiments in which we found that in neocortical areas (e.g., the parietal cortex) BrdU incorporation is reduced and appears to be delayed in comparison with the EC and other parts of the allocortex (unpublished data; Supplementary Figure 8).

The transient proliferative response in the EC opposite to the CSD was unexpected, as CSD typically do not cross the midline. However, the lateralization of CSD does not exclude functional consequences in the contralateral hemisphere. Cortical spreading depolarization-related changes in neuronal activity may be transferred via transhemispheric commissural connections (i.e., transcallosal diaschisis). This idea is supported by recent reports showing CSD-induced suppression of spontaneous spike rates and EEG spectral power in the bilateral cortex, whereas classic CSD-related changes in direct current potential, PO_2, and cortical blood flow kept restricted to the ipsilateral hemisphere.[25]

Which mechanisms may account for the observed glial responsiveness to CSD? There is a plenty of factors influencing activity and proliferation of glial cells, many of them also being expressed after CSD. For example, CSD is associated with a transient depolarization of neurons and glia, dramatic alterations in intracellular and extracellular ion concentrations (e.g., an increase in $[K^+]$), and the release of multiple neurotransmitters like glutamate and ATP.[1] In return, all three glia populations that have been examined in the present study express purinergic receptors of the P2X and P2Y type[26] as well as ionotropic and metabotropic glutamatergic receptors.[27–29] Moreover, NG2 glia receive direct synaptic inputs from neighboring neurons,[30] and microglia as well as astrocytes are sensitive to fluctuations in $[K^+]_o$.[31,32] Additionally, the ionic imbalances that accompany CSD cause a transient swelling of neurons and glia. Microglial cells are able to sense these changes by volume-regulated Cl^- channels, which may contribute to the regulation of cell division.[28] Furthermore, CSD initiates expression and release of cytokines and growth factors, with many of them having the potential to trigger gliosis.[11,33] For example, CSD increases CCL2, which drives the activation and division of microglia,[34] IL-6 that acts as mitogen for astrocytes,[35] and BDNF which has a role in the proliferation of NG2 cells and microglia.[36,37]

There are two factors related to our model that need to be addressed because they may contribute to the observed gliosis. First, KCl applied to the dura could diffuse into the brain parenchyma and by itself activate glia.[31,32] However, the minimum distance between the KCl application site and the EC was 7 to 8 mm making a pure diffusion effect unlikely. Supportingly, as mentioned above, cortical areas more close to the KCl application site (e.g., the parietal cortex) showed even less cytogenesis than the EC (Supplementary Figure 8). Second, hyperosmolar KCl induced necrotic lesions at the application site (Supplementary Figure 9A).[10,13] However, this focal tissue necrosis was also present in the controls after equimolar NaCl application, although less extensive, where it did not induce glial activation. Furthermore, we could not find any positive correlation between the lesion volume and the number of newborn cells (Supplementary Figure 9B), making it unlikely that gliosis was induced by the lesion itself.

The functional relevance and clinical implications of CSD-induced gliosis remain to be determined. Generally, our data corroborate the assumption that CSD contributes to reactive gliosis observed throughout remote ipsilateral cortex after acute brain injuries like stroke and traumatic brain injury. Whether these changes contribute to the progression of damage or neuroprotection and repair mechanisms remains open. Astrocytes and microglia carry a variety of different functions and their activation may have both, deleterious and protective consequences depending on context and activation state. Among other functions, astrocytes (1) remove glutamate, potassium, and free radicals from the extracellular space and dissipate them through astrocytic syncytium (spatial buffering), thus preventing detrimental accumulation of these factors; (2) store energy substrates (glycogen, lactate) which can be provided to neurons during periods of glucose deprivation; (3) release neurotrophic factors; and (4) maintain the integrity of the neurovascular unit and participate in control of local blood flow.[8,29] Microglia are able to (1) release neurotrophins; (2) uptake glutamate, which helps preventing glutamate-related excitotoxicity; and (3) remove cellular debris and inflammatory cells by phagocytosis.[16] Given these functions it is likely that an enlarged pool of mildly activated glia increases the capacity of brain tissue to suppress subsequent CSD events, to respond to severe injuries and to serve protective functions immediately, which might account for CSD-induced ischemic tolerance.[38,39] Furthermore, the CSD-induced gliosis may contribute to the increase in cortical thickness recently found in migraine patients,[40] although it can be assumed that the magnitude of gliosis is smaller in migraineurs, as an aura is associated to one rather than to a cluster of CSD.

Together, our data suggest that CSD have long-lasting consequences on the cellular composition of the healthy brain which almost certainly contribute to the etiopathology of CSD-related disorders like trauma, ischemic, and hemorrhagic stroke.

DISCLOSURE/CONFLICT OF INTEREST

The authors declare no conflict of interest.

REFERENCES

1 Somjen GG. Mechanisms of spreading depression and hypoxic spreading depression-like depolarization. *Physiol Rev* 2001; **81**: 1065–1096.

2 Dreier JP. The role of spreading depression, spreading depolarization and spreading ischemia in neurological disease. *Nat Med* 2011; **17**: 439–447.

3 Lauritzen M, Dreier JP, Fabricius M, Hartings JA, Graf R, Strong AJ *et al*. Clinical relevance of cortical spreading depression in neurological disorders: migraine, malignant stroke, subarachnoid and intracranial hemorrhage, and traumatic brain injury. *J Cereb Blood Flow Metab* 2011; **31**: 17–35.

4 Tamura Y, Kataoka Y, Cui Y, Yamada H. Cellular proliferation in the cerebral cortex following neural excitation in rats. *Neurosci Res* 2004; **50**: 129–133.

5 Block F, Dihne M, Loos M. Inflammation in areas of remote changes following focal brain lesion. *Prog Neurobiol* 2005; **75**: 342–365.

6 Schroeter M, Jander S, Witte OW, Stoll G. Heterogeneity of the microglial response in photochemically induced focal ischemia of the rat cerebral cortex. *Neuroscience* 1999; **89**: 1367–1377.

7 Urrea C, Castellanos DA, Sagen J, Tsoulfas P, Bramlett HM, Dietrich WD *et al*. Widespread cellular proliferation and focal neurogenesis after traumatic brain injury in the rat. *Restor Neurol Neurosci* 2007; **25**: 65–76.

8 Sofroniew MV, Vinters HV. Astrocytes: biology and pathology. *Acta Neuropathol* 2010; **119**: 7–35.

9 Kokaia Z, Lindvall O. Neurogenesis after ischaemic brain insults. *Curr Opin Neurobiol* 2003; **13**: 127–132.

10 Urbach A, Redecker C, Witte OW. Induction of neurogenesis in the adult dentate gyrus by cortical spreading depression. *Stroke* 2008; **39**: 3064–3072.

11 Urbach A, Bruehl C, Witte OW. Microarray-based long-term detection of genes differentially expressed after cortical spreading depression. *Eur J Neurosci* 2006; **24**: 841–856.

12 Holmin S, von Gertten C, Sandberg-Nordqvist AC, Lendahl U, Mathiesen T. Induction of astrocytic nestin expression by depolarization in rats. *Neurosci Lett* 2001; **314**: 151–155.

13 Kraig RP, Dong LM, Thisted R, Jaeger CB. Spreading depression increases immunohistochemical staining of glial fibrillary acidic protein. *J Neurosci* 1991; **11**: 2187–2198.

582

14 Xue JH, Yanamoto H, Nakajo Y, Tohnai N, Nakano Y, Hori T *et al.* Induced spreading depression evokes cell division of astrocytes in the subpial zone, generating neural precursor-like cells and new immature neurons in the adult cerebral cortex. *Stroke* 2009; **40**: e606–e613.

15 Tamura Y, Eguchi A, Jin G, Sami MM, Kataoka Y. Cortical spreading depression shifts cell fate determination of progenitor cells in the adult cortex. *J Cereb Blood Flow Metab* 2012; **32**: 1879–1887.

16 Hanisch UK, Kettenmann H. Microglia: active sensor and versatile effector cells in the normal and pathologic brain. *Nat Neurosci* 2007; **10**: 1387–1394.

17 Gehrmann J, Mies G, Bonnekoh P, Banati R, Iijima T, Kreutzberg GW *et al.* Microglial reaction in the rat cerebral cortex induced by cortical spreading depression. *Brain Pathol* 1993; **3**: 11–17.

18 Ge WP, Miyawaki A, Gage FH, Jan YN, Jan LY. Local generation of glia is a major astrocyte source in postnatal cortex. *Nature* 2012; **484**: 376–380.

19 Zhu X, Bergles DE, Nishiyama A. NG2 cells generate both oligodendrocytes and gray matter astrocytes. *Development* 2008; **135**: 145–157.

20 Dawson MR, Polito A, Levine JM, Reynolds R. NG2-expressing glial progenitor cells: an abundant and widespread population of cycling cells in the adult rat CNS. *Mol Cell Neurosci* 2003; **24**: 476–488.

21 Komitova M, Perfilieva E, Mattsson B, Eriksson PS, Johansson BB. Enriched environment after focal cortical ischemia enhances the generation of astroglia and NG2 positive polydendrocytes in adult rat neocortex. *Exp Neurol* 2006; **199**: 113–121.

22 Tamura Y, Kataoka Y, Cui Y, Takamori Y, Watanabe Y, Yamada H *et al.* Multi-directional differentiation of doublecortin- and NG2-immunopositive progenitor cells in the adult rat neocortex in vivo. *Eur J Neurosci* 2007; **25**: 3489–3498.

23 Gould E. How widespread is adult neurogenesis in mammals? *Nat Rev Neurosci* 2007; **8**: 481–488.

24 Yanamoto H, Miyamoto S, Tohnai N, Nagata I, Xue JH, Nakano Y *et al.* Induced spreading depression activates persistent neurogenesis in the subventricular zone, generating cells with markers for divided and early committed neurons in the caudate putamen and cortex. *Stroke* 2005; **36**: 1544–1550.

25 Unekawa M, Tomita Y, Toriumi H, Masamoto K, Kanno I, Suzuki N *et al.* Potassium-induced cortical spreading depression bilaterally suppresses the electroencephalogram but only ipsilaterally affects red blood cell velocity in intraparenchymal capillaries. *J Neurosci Res* 2013; **91**: 578–584.

26 Verkhratsky A, Krishtal OA, Burnstock G. Purinoceptors on neuroglia. *Mol Neurobiol* 2009; **39**: 190–208.

27 Hamilton N, Vayro S, Wigley R, Butt AM. Axons and astrocytes release ATP and glutamate to evoke calcium signals in NG2-glia. *Glia* 2010; **58**: 66–79.

28 Kettenmann H, Hanisch UK, Noda M, Verkhratsky A. Physiology of microglia. *Physiol Rev* 2010; **91**: 461–553.

29 Seifert G, Schilling K, Steinhauser C. Astrocyte dysfunction in neurological disorders: a molecular perspective. *Nat Rev Neurosci* 2006; **7**: 194–206.

30 Bergles DE, Roberts JD, Somogyi P, Jahr CE. Glutamatergic synapses on oligodendrocyte precursor cells in the hippocampus. *Nature* 2000; **405**: 187–191.

31 Abraham H, Losonczy A, Czeh G, Lazar G. Rapid activation of microglial cells by hypoxia, kainic acid, and potassium ions in slice preparations of the rat hippocampus. *Brain Res* 2001; **906**: 115–126.

32 Del Bigio MR, Omara F, Fedoroff S. Astrocyte proliferation in culture following exposure to potassium ion. *Neuroreport* 1994; **5**: 639–641.

33 Thompson CS, Hakim AM. Cortical spreading depression modifies components of the inflammatory cascade. *Mol Neurobiol* 2005; **32**: 51–58.

34 Hinojosa AE, Garcia-Bueno B, Leza JC, Madrigal JL. CCL2/MCP-1 modulation of microglial activation and proliferation. *J Neuroinflammation* 2011; **8**: 77.

35 Selmaj KW, Farooq M, Norton WT, Raine CS, Brosnan CF. Proliferation of astrocytes in vitro in response to cytokines. A primary role for tumor necrosis factor. *J Immunol* 1990; **144**: 129–135.

36 Vondran MW, Clinton-Luke P, Honeywell JZ, Dreyfus CF. BDNF+/− mice exhibit deficits in oligodendrocyte lineage cells of the basal forebrain. *Glia* **58**: 848–856.

37 Gomes C, Ferreira R, George J, Sanches R, Rodrigues DI, Goncalves N *et al.* Activation of microglial cells triggers a release of brain-derived neurotrophic factor (BDNF) inducing their proliferation in an adenosine A2A receptor-dependent manner: A2A receptor blockade prevents BDNF release and proliferation of microglia. *J Neuroinflammation* **10**: 16.

38 Muramatsu H, Kariko K, Welsh FA. Induction of tolerance to focal ischemia in rat brain: dissociation between cortical lesioning and spreading depression. *J Cereb Blood Flow Metab* 2004; **24**: 1167–1171.

39 Matsushima K, Schmidt-Kastner R, Hogan MJ, Hakim AM. Cortical spreading depression activates trophic factor expression in neurons and astrocytes and protects against subsequent focal brain ischemia. *Brain Res* 1998; **807**: 47–60.

40 DaSilva AF, Granziera C, Snyder J, Hadjikhani N. Thickening in the somatosensory cortex of patients with migraine. *Neurology* 2007; **69**: 1990–1995.

Supplementary Information accompanies the paper on the Journal of Cerebral Blood Flow & Metabolism website (http://www.nature.com/jcbfm)